

Sr_{0.9}K_{0.1}Zn_{1.8}Mn_{0.2}As₂: a ferromagnetic semiconductor with colossal magnetoresistance

Xiaojun Yang,¹ Qian Chen,¹ Yupeng Li,¹ Zhen Wang,¹ Jinke Bao,¹ Yuke Li,² Qian Tao,¹ Guanghan Cao,¹ and Zhu-an Xu^{1,*}

¹*Department of Physics and State Key Laboratory of Silicon Materials, Zhejiang University, Hangzhou 310027, China*

²*Department of Physics, Hangzhou Normal University, Hangzhou 310036, China*

(Dated: September 10, 2014)

A bulk diluted magnetic semiconductor (Sr,K)(Zn,Mn)₂As₂ was synthesized with decoupled charge and spin doping. It has a hexagonal CaAl₂Si₂-type structure with the (Zn,Mn)₂As₂ layer forming a honeycomb-like network. Magnetization measurements show that the sample undergoes a ferromagnetic transition with a Curie temperature of 12 K and magnetic moment reaches about 1.5 μ_B /Mn under $\mu_0 H = 5$ T and $T = 2$ K. Surprisingly, a colossal negative magnetoresistance, defined as $[\rho(H) - \rho(0)]/\rho(0)$, up to -38% under a low field of $\mu_0 H = 0.1$ T and to -99.8% under $\mu_0 H = 5$ T, was observed at $T = 2$ K. The colossal magnetoresistance can be explained based on the Anderson localization theory.

PACS numbers: 75.50.Pp; 75.30.Kz; 75.47.Gk

I. INTRODUCTION

Combining semiconductor and magnetism, diluted magnetic semiconductors (DMS) which possess both spin and charge degrees of freedom have attracted much attention because such DMS materials not only exhibit substantial novel phenomena such as quantum Hall effects, semiconductor lasers and single-electron charging, but also bring about numerous applications in sensors, memories as well as spintronics¹⁻⁵. However, the III-V based DMS materials, represented by (Ga,Mn)As, obtained by heterovalent substitution of Mn²⁺ for Ga³⁺, are only available as thin films due to the limited chemical solubility of manganese in bulk GaAs ($< 1\%$), and lack independently controlling of local moment and carrier densities^{6,7}.

The I-II-V based Li(Zn,Mn)As was theoretically proposed to be an n-type DMS and experimentally synthesized as a bulk p-type DMS material with Curie temperature (T_C) of 50 K^{6,8}. In this bulk system charge and spin concentrations can be tuned separately via Li off-stoichiometry and the isovalent substitution of Mn²⁺ for Zn²⁺, and the solubility of Mn is significantly enhanced. Actually, only in a limited number of DMS systems the concentration of acceptor and Mn impurity (i.e., magnetic moment) can be tuned independently⁹⁻¹¹. Inspired by the rapid development of iron-based superconductors¹²⁻¹⁴, a series of DMS systems based on the similar layered structure were found^{7,15-17}.

The so-called colossal magnetoresistance (CMR) is usually observed in manganites, where the complex and intimate link among magnetic structure, crystallographic structure and electrical resistivity makes it a focus of research interest¹⁸⁻²⁰. Materials exhibiting large MR can be exploited to enlarge the sensitivity of read/write heads of magnetic storage devices and thus to maximize the information density¹⁹. But magnetic fields of several tesla are typically required to obtain such a CMR effect, which limits the potential for applications^{21,22}. The CMR ef-

fect under a low field is highly required from viewpoint of practical use.

SrZn₂As₂ is a compound with hexagonal CaAl₂Si₂-type structure (shown in Fig. 1(a) and (b))²³, which belongs to P-3m1 (No.164) space group. The Zn₂As₂ layers form a honeycomb-like network. No detail study on the physical properties of SrZn₂As₂ has been reported yet. Attracting more and more attention, the honeycomb-like network is essential in recently extensively investigated topological insulators^{24,25}. Recently, a first honeycomb-lattice bulk DMS (Ba,K)(Cd,Mn)₂As₂ with $T_C \sim 16$ K²⁶ has been reported. In this Letter, we report successful synthesis of a honeycomb-lattice bulk DMS (Sr,K)(Zn,Mn)₂As₂ with $T_C \sim 12$ K and magnetic moment of about 1.5 μ_B /Mn under $\mu_0 H = 5$ T and $T = 2$ K. In this system, charge and spin degree of freedom can be controlled independently via K⁺ for Sr²⁺ and isovalent Mn²⁺ for Zn²⁺ substitution, respectively. Surprisingly, a large MR, defined as $[\rho(H) - \rho(0)]/\rho(0)$, up to -38% under a low field of $\mu_0 H = 0.1$ T and to -99.8% under $\mu_0 H = 5$ T at $T = 2$ K was observed. Only a limited number of systems (systems represented by (Ga,Mn)As and (La,Sr)MnO₃) exhibit such a remarkable CMR behavior^{5,18,27}. The colossal magnetoresistance can be explained based on the Anderson localization theory. Although T_C of this system may be too low for practical use, our work encourages people to explore colossal magnetoresistance in the other recently discovered bulk DMS materials, such as (Ba,K)(Zn, Mn)₂As₂¹⁵ and (La,Sr)(Cu,Mn)SO¹⁷ with much high Curie temperatures, which makes the recently discovered bulk DMSs truly appealing class of systems.

II. EXPERIMENTAL

The polycrystalline samples of (Sr,K)(Zn,Mn)₂As₂ were synthesized by solid state reaction method. All the starting materials, Sr granules, K lumps, and the powders of Zn, Mn and As are of high purity ($\geq 99.9\%$). As a

first step, SrAs was presynthesized by reacting stoichiometric Sr granules and As powder at 1123 K for 48 h, and KAs was presynthesized by heating stoichiometric K lumps and As powder with a ramping rate of 0.25 K/min to 773 K and kept at that temperature for 10 h. Then the resultants SrAs and KAs, and the powders of Zn, As and Mn were weighted according to their stoichiometric ratio and then fully ground in an agate mortar. The mixture was then pressed into pellets, heated in evacuated quartz tubes at 1223 K for 33 h, and finally furnace cooled to room temperature. The process was repeated once again in order to get the pure phase.

Powder x-ray diffraction (XRD) was performed at room temperature using a PANalytical x-ray diffractometer (Model EMPYREAN) with a monochromatic $\text{CuK}\alpha_1$ radiation. The electrical resistivity was measured by four-terminal method. The dc magnetization was measured on a Quantum Design magnetic property measurement system (MPMS-5). The magneto-resistance and Hall coefficient was measured using a Quantum-Design physical property measurement system (PPMS).

III. RESULTS AND DISCUSSION

Figure 1(c) shows the X-ray diffraction patterns of $(\text{Sr,K})(\text{Zn,Mn})_2\text{As}_2$. The crystal structure is also sketched in Fig. 1(a) and (b). The diffraction peaks of both SrZn_2As_2 and $\text{Sr}_{0.9}\text{K}_{0.1}\text{Zn}_{1.8}\text{Mn}_{0.2}\text{As}_2$ can be well indexed based on the P-3m1 (No.164) space group with a hexagonal CaAl_2Si_2 -type structure. The XRD patterns indicate that the samples are essentially single phase. The lattice parameters of the two samples were obtained by least-squares fit of more than 20 reflection peaks with the correction of zero shift, using space group of P-3m1 (No.164). The resulting room temperature lattice constants a and c are 4.223 Å and 7.270 Å, respectively for the SrZn_2As_2 parent compound, consistent with the previously reported values $a = 4.223$ Å and $c = 7.268$ Å²³. Upon K and Mn doping, the lattice constants of $\text{Sr}_{0.9}\text{K}_{0.1}\text{Zn}_{1.8}\text{Mn}_{0.2}\text{As}_2$ increase slightly to $a = 4.232$ Å and $c = 7.280$ Å, which is consistent with the fact that the ionic radius of the Mn^{2+} ion is larger than that of Zn^{2+} and the ionic radius of the K^+ ion is also larger than that of Sr^{2+} . As shown in Fig. 1(d), the Rietveld refinement of the $\text{Sr}_{0.9}\text{K}_{0.1}\text{Zn}_{1.8}\text{Mn}_{0.2}\text{As}_2$ sample based on the CaAl_2Si_2 -type structure shows that the calculated profile well matches the experimental data. The weighted reliable factor R_{wp} and the goodness of fit S are 12.8% and 1.27, respectively.

In Fig. 2(a), the temperature dependence of dc magnetization of $\text{Sr}_{0.9}\text{K}_{0.1}\text{Zn}_{1.8}\text{Mn}_{0.2}\text{As}_2$ is shown for both zero-field cooling (ZFC) and field-cooling (FC) procedures under $H = 1$ kOe and 10 Oe. No significant difference can be found between ZFC and FC data when the applied field $H = 1$ kOe. Below $(T_C) \sim 12$ K, an abrupt increase in magnetization can be observed, which is a signature of ferromagnetic order. In the inset of Fig. 2(a),

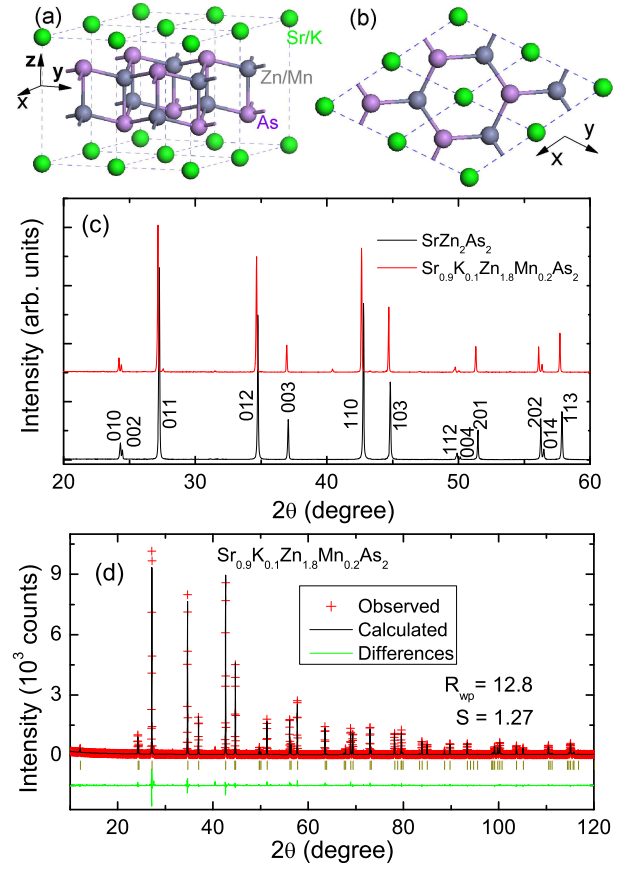


FIG. 1: (Color online) (a,b), The crystal structure of $(\text{Sr,K})(\text{Zn,Mn})_2\text{As}_2$. (c), Room-temperature XRD patterns of SrZn_2As_2 (lower curve) and $\text{Sr}_{0.9}\text{K}_{0.1}\text{Zn}_{1.8}\text{Mn}_{0.2}\text{As}_2$ (upper curve), indexed based on the P-3m1 (No.164) space group. (d), Rietveld refinement of the powder X-ray diffraction for the $\text{Sr}_{0.9}\text{K}_{0.1}\text{Zn}_{1.8}\text{Mn}_{0.2}\text{As}_2$ sample.

the data are shown in the plot of M^2 verse H/M (Arrot plot), which clearly indicates that the Curie temperature (T_C) is about 12 K. Under an applied field of 10 Oe, a bifurcation between ZFC and FC curves can be observed below the temperature $T_f = 6$ K, where T_f stands for the freezing temperature of individual spins or domain wall motion. As discussed in Ref.^{16,28}, the bifurcation of ZFC and FC curves and the hysteresis loops can be found not only in regular ferromagnets but also in spin glasses. In typical spin glass systems, the moment size is usually small, i.e., $\sim 0.01 \mu_B/\text{Mn}$ for the II-VI $(\text{Zn,Mn})\text{Se}$ or other typical diluted alloy spin glasses^{29–31}. Considering that the magnetic moment of our system is $0.22 \mu_B/\text{Mn}$ under a small field of $H = 10$ Oe and can reach $0.89 \mu_B/\text{Mn}$ under $H = 1000$ Oe, we tentatively assign it to a ferromagnetic ordering rather than a spin glass. The small magnetization anomaly at $T \sim 320$ K should be due to the traceable MnAs impurity phase,^{32,33} whose content is too small to be detected by X-ray diffraction. The large increase of magnetization and magnetoresistance (MR) below temperature of about 12 K cannot be

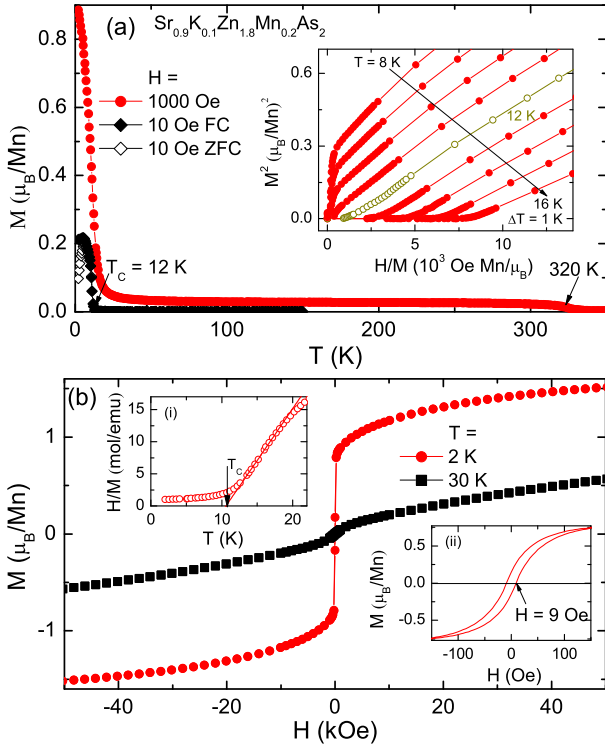


FIG. 2: (Color online) (a), Temperature dependence of dc magnetic susceptibility measured under $H = 1$ kOe and 10 Oe for $\text{Sr}_{0.9}\text{K}_{0.1}\text{Zn}_{1.8}\text{Mn}_{0.2}\text{As}_2$ with solid symbols standing for FC and open ones for ZFC. No significant difference can be found between ZFC and FC data when $H = 1$ kOe. The inset of (a) display plot of M^2 verse H/M (Arrott plot) at various temperatures. (b), Field dependence of magnetization measured at 2 K and 30 K. The inset of (b): (i) plot of H/M vs. T and the determination of the Curie temperature T_C is shown; (ii) the enlarged $M(H)$ curve.

attributed to the traceable MnAs impurity phase. In the inset (i) of Fig. 2(b), we plot H/M vs. T curve, which goes to zero at T_C (around 12 K), consistent with the Arrott plot

The magnetic field dependence of magnetization, i.e. $M(H)$ curves, of $\text{Sr}_{0.9}\text{K}_{0.1}\text{Zn}_{1.8}\text{Mn}_{0.2}\text{As}_2$ at $T = 2$ K and 30 K is shown in Fig. 2(b). At $T = 2$ K, the magnetization reaches $1.5 \mu_B/\text{Mn}$ under an applied field of $H = 50$ kOe, which is comparable with the result in $\text{Li}(\text{Mn}, \text{Zn})\text{As}$ ⁸ and $(\text{Ba}, \text{K})(\text{Zn}, \text{Mn})_2\text{As}_2$ ¹⁵. At $T = 30$ K, the $M(H)$ curve indicates that the sample is mainly in a paramagnetic state, but the traceable MnAs impurity with FM order can be observed. As shown in the inset (ii) of Fig. 2(b), the coercive field of $\text{Sr}_{0.9}\text{K}_{0.1}\text{Zn}_{1.8}\text{Mn}_{0.2}\text{As}_2$ is less than 10 Oe at $T = 2$ K. Such a coercive field is even smaller than that of $\text{Li}(\text{Mn}, \text{Zn})\text{As}$ (30-100 Oe)⁸, thus the material should be appealing in spin manipulation.

As shown in Fig. 3, for the SrZn_2As_2 parent compound, its resistivity clearly exhibits thermally activated behavior with decreasing temperature, and it increases beyond our measurement limitation below 70 K. The thermal activation energy (E_a) obtained by fitting with

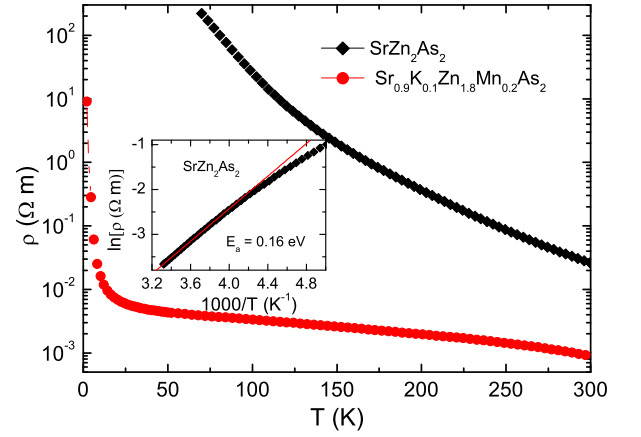


FIG. 3: (Color online) Temperature dependence of resistivity of SrZn_2As_2 and $\text{Sr}_{0.9}\text{K}_{0.1}\text{Zn}_{1.8}\text{Mn}_{0.2}\text{As}_2$. The inset: the $\ln \rho$ vs. $1/T$ plot for SrZn_2As_2 .

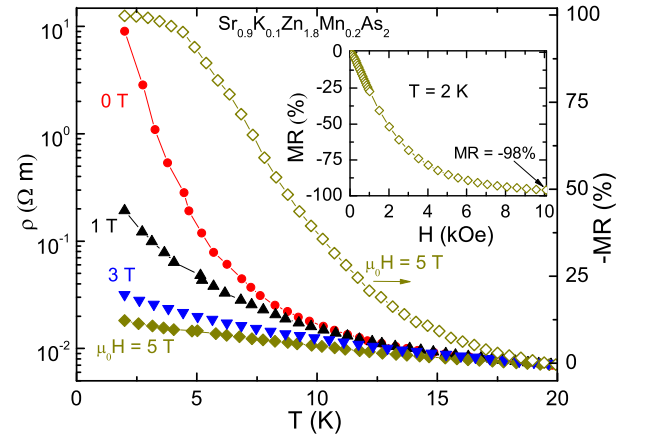


FIG. 4: (Color online) Temperature dependence of resistivity (left axis) under $\mu_0 H = 0, 1, 3, 5$ T and magnetoresistance (MR) (right axis), defined as $[\rho(H) - \rho(0)]/\rho(0)$, under $\mu_0 H = 5$ T for $\text{Sr}_{0.9}\text{K}_{0.1}\text{Zn}_{1.8}\text{Mn}_{0.2}\text{As}_2$. The inset displays the field dependence of MR at $T = 2$ K.

the thermal activation formula $\rho(T) = \rho_0 \exp(E_a/k_B T)$ for the temperature range from 250 to 300 K is 0.16 eV, as shown in the inset of Fig. 3. With 10% K-for-Sr substitution, p-type carriers can be introduced, and the resistivity of $\text{Sr}_{0.9}\text{K}_{0.1}\text{Zn}_{1.8}\text{Mn}_{0.2}\text{As}_2$ decreases rapidly compared with the SrZn_2As_2 parent compound, but it still increases with decreasing T , which should be due to the localization effect. The Hall effect of $\text{Sr}_{0.9}\text{K}_{0.1}\text{Zn}_{1.8}\text{Mn}_{0.2}\text{As}_2$ was also measured at $T = 300$ K and the charge carrier density is calculated to be $7.6 \times 10^{18}/\text{cm}^3$ by using the one-band model formula $R_H = 1/ne$. The positive Hall coefficient demonstrates that the hole type charge carrier is indeed dominant in the system, consistent with that 10% K-for-Sr substitution. However, the Hall coefficient is hard to measure at low temperatures, due to the extremely large resistivity.

We then measured the magnetoresistance(MR), de-

defined in the standard way as $[\rho(H) - \rho(0)]/\rho(0)$, (The magnitude of MR could be much larger if it is defined in the other way as $[\rho(H) - \rho(0)]/\rho(H)$), for $\text{Sr}_{0.9}\text{K}_{0.1}\text{Zn}_{1.8}\text{Mn}_{0.2}\text{As}_2$, as shown in Fig. 4. Without magnetic field, the resistivity is $9.0 \Omega \text{ m}$ at 2 K , which decreases rapidly with applied magnetic field. It reaches $5.84 \Omega \text{ m}$ under a low field of $\mu_0 H = 0.1 \text{ T}$ (MR = -38%), then to $0.19 \Omega \text{ m}$ under $\mu_0 H = 1 \text{ T}$ (MR = -98%), and even to $0.018 \Omega \text{ m}$ under $\mu_0 H = 5 \text{ T}$ (MR = -99.8%). Such a colossal magneto-resistance has only been observed in a limited number of systems (represented by (Ga,Mn)As and (La,Sr)MnO₃)^{5,18,27}. These materials have attracted much attention in the field of condensed matter physics.

In a typical manganite CMR system, i.e. (La,Sr)MnO₃, the scattering by fluctuating local magnetic moments plays an important role in the charge transport¹⁸, and thus MR is large around T_C , but it usually becomes smaller far below T_C ³⁴. However, CMR in $\text{Sr}_{0.9}\text{K}_{0.1}\text{Zn}_{1.8}\text{Mn}_{0.2}\text{As}_2$ keep increasing below T_C , which implies that the mechanism of CMR in this system could essentially be different. CMR in this system have two interesting features: (1) low coercivity field, (2) maximum in MR at temperatures far below T_C .

A similar negative magnetoresistance was observed in p-(Zn,Mn)Te, which also occurred below T_C and was thought to be related with the localization effect³⁵. On crossing the metal-insulator transition (MIT), the extended states become localized. However, according to the scaling theory of the MIT, their localization radius ξ decreases rather gradually from infinity at the MIT toward the Bohr radius deep in the insulator phase, so that on a length scale smaller than ξ , the wave function retains an extended character³⁶. Previous studies have demonstrated that ferromagnetic interactions can be mediated by the weakly localized holes showing an extended character^{36,37}.

In an Anderson localized system, the Fermi level is located on the localized side of the mobility edge. The application of a magnetic field introduces Zeeman shifts of each eigenstate dependent on spin directions, and the repopulation among Anderson localized states. For one of the spin subbands, the mobility edge moves toward the Fermi level. This results in a negative magnetoresistance because of the exponential dependence of the wave function ($\psi(r) \propto e^{-r/\xi}$) overlap on the localization length $\xi \propto (E_C - E)^\nu$, where E_C is the mobility edge and E is the energy of the localized state, ν is an exponent on the order of unity^{27,38}. We plot in Fig. 5 the magnetic field dependence of conductivity ($\sigma = 1/\rho$), and find a remarkable result that σ is linear in H for $10 \text{ kOe} \leq H \leq 50 \text{ kOe}$, i.e. $\sigma = C(H - H_c)$, with $C = 1.27 (\Omega \text{ m kOe})^{-1}$ and $H_c = 6.08 \text{ kOe}$. Based strictly on the concepts of localization, Abrahams *et al.*³⁹ and later Imry⁴⁰ pointed out, using scaling arguments, that $\sigma \propto (E_F(0) - E_C)^\nu$, where $\nu = 1$, which was also observed experimentally in several magnetic systems^{41,42}. Furthermore, it is known that, on the insulating side,

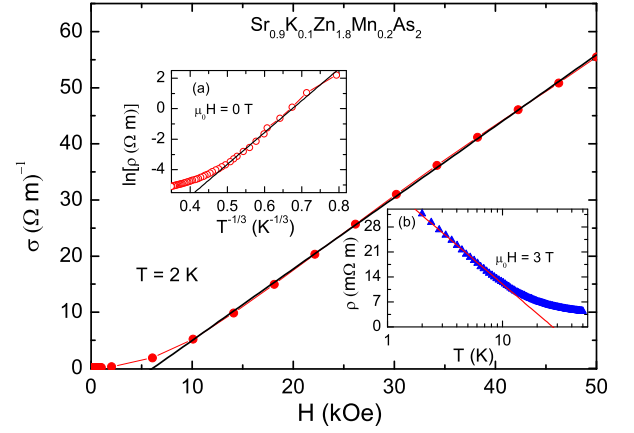


FIG. 5: (Color online) Magnetic field dependence of conductivity of $\text{Sr}_{0.9}\text{K}_{0.1}\text{Zn}_{1.8}\text{Mn}_{0.2}\text{As}_2$ at $T = 2 \text{ K}$. Inset (a): Resistivity of $\text{Sr}_{0.9}\text{K}_{0.1}\text{Zn}_{1.8}\text{Mn}_{0.2}\text{As}_2$ under zero magnetic field in $\ln \rho$ vs. $T^{-1/3}$ (2D-VRH) plot; (b) resistivity of under $\mu_0 H = 3 \text{ T}$ in ρ vs. $\log T$ plot.

$|E_F(0) - E_C|$ is linear in H for fields beyond approximately 6 kOe ^{41?}. We argue that $E_F(0) - E_C \geq 0$ in our case, and then $\sigma \propto (E_F(0) - E_C)^\nu \equiv C(H - H_c)^\nu$. Therefore, $\nu = 1$ observed in the present MR data may be compared directly to the exponents derived from the scaling theories⁴¹.

Exhibiting rapid increase at low temperatures, the resistivity can be roughly fit with $\rho(T) = Ce^{(T_0/T)^{1/3}}$ under $\mu_0 H = 0 \text{ T}$ (shown in the inset (a) of Fig. 5), which should be a typical behavior of Anderson insulators and known as the two-dimensional variable range hopping (2D-VRH)⁴⁴, stemming from the random potential scattering contributed by large numbers of disorders or defects. Magnetic field can align the magnetic moments and reduce the disorder of the system, and then resistivity exhibits the $\rho \propto -\log T$ behavior when the applied field $\mu_0 H \geq 3 \text{ T}$ (shown in the inset (b) of Fig. 5), which might be attributed to quantum correlations to the conductivity in weakly localized regime^{37,42,45}. All the results indicate that our studied system can be well described by the localization theories, and the negative CMR could be understood based on the Anderson localization.

Since most applications of MR effect require operating magnetic fields of less than several hundreds of Oe, to reduce the required magnetic field for CMR in manganites has been a major goal^{21,22}. In the studied $\text{Sr}_{0.9}\text{K}_{0.1}\text{Zn}_{1.8}\text{Mn}_{0.2}\text{As}_2$ system, MR reaches -38% only under an applied field of 1000 Oe . The low field MR may stem from the spin-dependent scattering at domain walls or grain boundaries in our poly-crystalline sample^{21,22}. An external field can align the magnetic domains, and thus the spin-dependent scattering will be reduced, resulting in a negative MR. Meanwhile, under high magnetic field, based on the the Anderson localization theory, the high magnetic field causes a delocalization effect, and

thus a negative colossal magnetoresistance is induced.

It should also be mentioned that the CMR effect is often accompanied by a metal-insulator phase transition induced by applying magnetic field near magnetic order temperatures as observed in III-V based (Ga,Mn)As and (In,Mn)As^{46–48}. However, no such metal-insulator phase transition is observed in Sr_{0.9}K_{0.1}Zn_{1.8}Mn_{0.2}As₂ or a similar system (Ba, K)(Cd, Mn)₂As₂²⁶. It is interesting whether a metal-insulator phase transition could be induced by applying an even higher magnetic field in these systems.

IV. CONCLUDING REMARKS

In summary, we have successfully prepared a bulk hexagonal DMS, (Sr,K)(Zn,Mn)₂As₂, with T_C of 12 K, and magnetic moment reaches about 1.5 μ_B /Mn under $\mu_0 H = 5$ T and $T = 2$ K. It is a soft magnet with a relatively small coercive field of less than 10 Oe. A low-

field CMR, defined as $[\rho(H) - \rho(0)]/\rho(0)$, reaches -38% under $\mu_0 H = 0.1$ T and up to -99.8% under $\mu_0 H = 5$ T. Further studies suggest that the Anderson delocalization due to applying magnetic field may account for the observed CMR effect. With decoupled charge and spin doping, the hexagonal (Sr,K)(Zn,Mn)₂As₂ combines semiconductor, ferromagnetism and colossal magnetoresistance, which makes it an appealing system.

Acknowledgments

This work is supported by the National Basic Research Program of China (Grant Nos. 2011CBA00103 and 2012CB821404), NSF of China (Contract Nos. 11174247 and U1332209), Specialized Research Fund for the Doctoral Program of Higher Education (Grant No. 20100101110004), and the Zhejiang Provincial Natural Science Foundation of China (Grant. No. Y6100216).

-
- * Electronic address: zhuan@zju.edu.cn
- ¹ H. Ohno, Science **281**, 951 (1998).
 - ² I. Žutić, J. Fabian, and S. Das Sarma. Rev. Mod. Phys. **76**, 323 (2004).
 - ³ T. Dietl, H. Ohno, F. Matsukura, J. Cibert, and D. Fermand, Science **287**, 1019 (2000).
 - ⁴ T. Dietl, Nature Mater. **9**, 965 (2010).
 - ⁵ H. Ohno, A. Shen, F. Matsukura, A. Oiwa, A. Endo, S. Katsumoto, and Y. Iye, Appl. Phys. Lett. **69**, 363 (1996).
 - ⁶ J. Mašek, J. Kudrnovský, F. Máca, B. L. Gallagher, R. P. Campion, D. H. Gregory, and T. Jungwirth, Phys. Rev. Lett. **98**, 067202 (2007).
 - ⁷ Z. Deng, K. Zhao, B. Gu, W. Han, J. L. Zhu, X. C. Wang, X. Li, Q. Q. Liu, R. C. Yu, T. Goko, B. Frandsen, L. Liu, J. Zhang, Y. Wang, F. L. Ning, S. Maekawa, Y. J. Uemura, and C. Q. Jin, Phys. Rev. B **88**, 081203(R) (2013).
 - ⁸ Z. Deng, C. Q. Jin, Q. Q. Liu, X. C. Wang, J. L. Zhu, S. M. Feng, L. C. Chen, R. C. Yu, C. Arguello, T. Goko, F. Ning, J. Zhang, Y. Wang, A. A. Aczel, T. Munsie, T. J. Williams, G. M. Luke, T. Kakeshita, S. Uchida, W. Higemoto, T. U. Ito, Bo Gu, S. Maekawa, G. D. Morris, and Y. J. Uemura, Nat. Commun. **2**, 422 (2011).
 - ⁹ T. Story, R. R. Galazka, R. B. Frankel, and P. A. Wolff, Phys. Rev. Lett. **56**, 777 (1986).
 - ¹⁰ A. Haury, A. Wasiela, A. Arnoult, J. Cibert, S. Tatarenko, T. Dietl, and Y. M. d'Aubigné, Phys. Rev. Lett. **79**, 511 (1997).
 - ¹¹ D. Ferrand, J. Cibert, C. Bourgognon, S. Tatarenko, A. Wasiela, G. Fishman, A. Bonanni, H. Sitter, S. Kolečnik, J. Jaroszyński, A. Barcz, and T. Dietl, J. Cryst. Growth, **214/215**, 387 (2000).
 - ¹² Y. Kamihara, T. Watanabe, M. Hirano, and H. Hosono, J. Am. Chem. Soc. **130**, 3296 (2008).
 - ¹³ C. Wang, L. J. Li, S. Chi, Z. W. Zhu, Z. Ren, Y. K. Li, Y. T. Wang, X. Lin, Y. K. Luo, S. Jiang, X. F. Xu, G. H. Cao, and Z. A. Xu, Europhys. Lett. **83**, 67006 (2008).
 - ¹⁴ M. Rotter, M. Tegel, and D. Johrendt, Phys. Rev. Lett. **101**, 107006 (2008).
 - ¹⁵ K. Zhao, Z. Deng, X. C. Wang, W. Han, J. L. Zhu, X. Li, Q. Q. Liu, R. C. Yu, T. Goko, B. Frandsen, L. Liu, F. Ning, Y. J. Uemura, H. Dabkowska, G. M. Luke, H. Luetkens, E. Morenzoni, S. R. Dunsiger, A. Senyshyn, P. Boni, and C. Q. Jin, Nat. Commun. **4**, 1442 (2013).
 - ¹⁶ C. Ding, H. Man, C. Qin, J. Lu, Y. Sun, Q. Wang, B. Yu, C. Feng, T. Goko, C. J. Arguello, L. Liu, B. A. Frandsen, Y. J. Uemura, H. Wang, H. Luetkens, E. Morenzoni, W. Han, C. Q. Jin, T. Munsie, T. J. Williams, R. M. D'Ortenzio, T. Medina, G. M. Luke, T. Imai, and F. L. Ning, Phys. Rev. B **88**, 041102(R) (2013).
 - ¹⁷ X. Yang, Y. Li, C. Shen, B. Si, Y. Sun, Q. Tao, G. Cao and Z. Xu, and F. Zhang, Appl. Phys. Lett. **103**, 022410 (2013).
 - ¹⁸ A. Urushibara, Y. Moritomo, T. Arima, A. Asamitsu, G. Kido, Y. Tokura, Phys. Rev. B **51**, 14103 (1995).
 - ¹⁹ N. Manyala, Y. Sidis, J. F. DiTusa, G. Aeppli, D. P. Young, and Z. Fisk, Nature **404**, 581 (2000).
 - ²⁰ S. Jin, T. H. Tiefel, M. McCormack, R. A. Fastnacht, R. Ramesh, and L. H. Chen, science **264**, 413 (1994).
 - ²¹ N. D. Mathure, G. Burnell, S. P. Isaac, T. J. Jackson, B. S. Teo, J. L. Macmanus-driscoll, L. F. Cohen, J. E. Evetts, and M. G. Blamire, Nature **387**, 266 (1997).
 - ²² H. S. Wang, and Qi Li, Appl. Phys. Lett. **73**, 2360 (1998).
 - ²³ A. Mewis, Z. Naturforsch, B: Anorg. Chem., Org. Chem. **35**, 939 (1980).
 - ²⁴ H. Zhang, C. Liu, X. Qi, Xi Dai, Z. Fang, and S. Zhang, Nature Physics **5**, 438 (2009).
 - ²⁵ M. Wang, C. Liu, J. Xu, F. Yang, L. Miao, M. Yao, C. L. Gao, C. Shen, X. Ma, X. Chen, Z. Xu, Y. Liu, S. Zhang, D. Qian, J. Jia, and Q. Xue, Science **336**, 52 (2012).
 - ²⁶ X. J. Yang, Y. K. Li, P. Zhang, H. Jiang, Q. Chen, C. M. Feng, C. Cao, J. H. Dai, Q. Tao, G. H. Cao, and Z. Xu, J. Appl. Phys. **114**, 223905 (2013).
 - ²⁷ A. Oiwa, S. Katsumoto, A. Endo, M. Hirasawa, Y. Iye, H. Ohno, F. Matsukura, A. Shen, and Y. Sugawara, Solid State Commun. **103**, 209 (1997).
 - ²⁸ H. Man, C. Qin, C. Ding, Q. Wang, X. Gong, S. Guo, H.

- Wang, B. Chen, F. L. Ning, Europhys. Lett. **105**, 67004 (2014).
- ²⁹ J.L. Tholence, R. and Tournier, J. Phys. (Paris) **35**, C4-229(1974).
- ³⁰ P. Monod, J.J. Prejean, and B. Tissier, J. Appl. Phys. **50**, 7324 (1979).
- ³¹ J.J. Prejean, M. Joliclerc, and P. Monod, J. Phys. (Paris) **41**1980427.
- ³² C. Guillaud, J. Phys. Radium **12**, 223 (1951).
- ³³ H. Wadaa, Y. Tanabe, Appl. Phys. Lett. **79**, 3302 (2001).
- ³⁴ M. E. Fisher, and J. S. Langer, Phys. Rev. Lett. **20**, 665 (1968).
- ³⁵ Ferrand D., Cibert J., Wasiela A., Bourgognon C., Tatarenko S., Fishman G., Andrearczyk T., Jaroszyński J., Koleśnik S., Dietl T., Barbara B., Dufeu D. Phys. Rev. B **63** 085201, (2001).
- ³⁶ Dietl T., Ohno H., Matsukura F., Cibert J., Ferrand D. Science **287** 1019, (2000).
- ³⁷ T. Dietl, J. Phys. Soc. Jpn. **77** 031005, (2008).
- ³⁸ H. Fukuyama, and K. Yosida, J. Phys. Soc. Jpn, **46**, 102 (1979).
- ³⁹ E. Abrahams, P. W. Anderson, D. C. Licciardello, and T. V. Bamakrishnan, Phys. Rev. Lett. **42**, 673 (1979).
- ⁴⁰ Y. Imry, Phys. Rev. Lett. **44**, 469 (1980).
- ⁴¹ S. von Molnar, A. Briggs, J. Flouquet, and G. Remenyi, Phys. Rev. Lett. **51**, 706 (1983).
- ⁴² T. Wojtowicz, T. Dietl, M. Sawicki, W. Plesiewicz, and J. Jaroszyński, Phys. Rev. Lett. **56**, 2419 (1986).
- ⁴³ T. Penney, F. Holtzberg, L. J. Tao, and S. von Molnar, in *Magnetism and Magnetic Materials* - 1973, edited by C. D. Graham, Jr., and J. J. Rhyne, AIP Conference Proceedings No. 18 (American Institute of Physics, New York, 1974), p. 908.
- ⁴⁴ P. V. E. McLintock, D. J. Meredith, and J. K. Wigmore, *Matter at Low Temperatures* (Blackie, Glasgow, 1984), p. 82.
- ⁴⁵ F. Matsukura, M. Sawicki, T. Dietl, D. Chiba, and H. Ohno, Physica E **21**, 1032 (2004).
- ⁴⁶ S. R. Dunsiger, J. P. Carlo, T. Goko, G. Nieuwenhuys, T. Prokscha, A. Suter, E. Morenzoni, D. Chiba, Y. Nishitani, T. Tanikawa, F. Matsukura, H. Ohno, J. Ohe, S. Maekawa, and Y. J. Uemura, Nature Mater. **9**, 299 (2010).
- ⁴⁷ H. Ohno, H. Munekata, T. Penney, S. vonMolnar, and L. L. Chang, Phys. Rev. Lett. **68**, 2664 (1992).
- ⁴⁸ H. Ohno, J. Magn. Magn. Mater. **200**, 110 (1999).